

USING A NONANALYTICAL APPROACH TO MODEL NONLINEAR DYNAMICS IN PHOTOSYNTHESIS AT THE PHOTOSYSTEM LEVEL¹

Samuel R. Laney,^{2,3} Ricardo M. Letelier, and Mark R. Abbott

College of Oceanic & Atmospheric Sciences, Oregon State University, Corvallis, Oregon 97331-5503, USA

Nonlinear dynamics in photon capture and uptake at the photosystem level may have a strong effect on photosynthetic yield. However, the magnitude of such effects is difficult to estimate theoretically because nonlinear systems often cannot be represented accurately using equations. A nonanalytical simulation was developed that used a simple decision tree and Monte Carlo methods, instead of equations, to model how a population of photosystems absorbs and utilizes photons from an ambient light field. This simulation replicated realistic kinetics in the closure and variable fluorescence yield of PSII on the single-turnover timescale, as well as the saturating behavior in light-driven electron flow that is observed in nature with increasing irradiance. This simulation indicated that the transfer of absorbed photon energy among PSII units can introduce strong nonlinear enhancement in light-driven electron flow. However, this effect was seen only in populations with particular photosynthetic states as determined by physiological properties of PSII. Other populations with the same degree of energy transfer but with different photosynthetic states exhibited little enhancement in electron flow and, in some cases, a reduction. This nonanalytical approach provides a simple means to quantify theoretically how nonlinear dynamics in photosynthesis arise at the photosystem level and how these dynamics may act to enhance or constrain photosynthetic rates and yields. Such simulations can provide quantitative insight into different physiological bases of nonlinear light-harvesting dynamics and identify those that would have the strongest theoretical influence and thus warrant closer experimental examination.

Key index words: model; Monte Carlo; nonanalytical; nonlinear; photosynthesis; photosystem; phytoplankton; PSII; simulation

Abbreviations: FRR (FRRF), fast repetition rate (fluorometer); RCII, reaction center II

Several analytical equations have been used to parameterize the photosynthesis-irradiance ($P-E$) relationship of plants and algae. These include rectangular hyperbolae (Maskell 1928, Baly 1935, Thornley 1998), hyperbolic tangents (Jassby and Platt 1976), quadratics (Smith 1936), exponentials (Webb et al. 1974), and other more complex forms (Bannister 1979, Thornley 1998). These equations all express the saturation of P with increasing E that is observed in nature and are useful in ecological models for characterizing the approximate photosynthetic state of plants and algae. Yet these equations do not provide a mechanistic description of the specific physiological factors that control the $P-E$ relationship. The parameters in these equations are purely empirical and lack concise physiological definitions (Abbott 1993).

A mechanistic model for the saturating $P-E$ relationship can also be derived from physiological first principles by using target theory, which describes photon capture and uptake at the photosystem level in terms of two physiological properties of photosystems: their mean functional cross-section (σ) to absorb a photon and the timescale (τ) with which electron acceptors drain this photon energy away (Dubinsky et al. 1986, Cullen 1990). These two properties act jointly to establish a dynamical balance between the flux of energy into and out of a population of photosystems (Han 2001). In theory, plants or algae are optimally adjusted for photon capture when the rate of exciton trapping by a population of photosystems matches the rate of electron transport (Falkowski and Raven 1997). Conversely, when these rates are out of balance, this energy flow is less than optimal in a dynamical sense. In empirical $P-E$ relationships, this balance is closely related to the difference between the ambient irradiance and E_K , an idealized irradiance that represents an average acclimation state below and above which a photoautotroph is light limited or light saturated, respectively. In a target theory model, an analogous parameter in a dynamical sense is the inverse product of σ and τ (Falkowski 1992).

$$\text{"dynamical" } E_K \equiv \frac{10^6}{6.022 \cdot 10^{23} \cdot (\sigma \cdot 10^{-20}) \cdot (\tau \cdot 10^{-3})} \quad (1)$$

¹Received 4 September 2007. Accepted 2 October 2008.

²Author for correspondence: e-mail slaney@whoi.edu.

³Present address: Biology Department, Woods Hole Oceanographic Institution, Massachusetts 02543, USA.

This “dynamical” E_K represents the threshold irradiance at which the rate of photon capture by a population of photosystems exceeds the rate by which this energy is transported away by electron acceptors. Here, constants convert the units of $(\sigma \cdot \tau)^{-1}$ into those of irradiance ($\mu\text{mol quanta} \cdot \text{m}^{-2} \cdot \text{s}^{-1}$) so that this dynamical E_K can be compared to the ambient irradiance. This scaling provides a means to determine how dynamically well matched the photosystems of a plant or alga are to the current incident photon flux.

Mechanistic models for the P - E relationship like those derived using target theory provide important mechanistic insight into how the structure and function of photosystems affect the dynamics of light harvesting and photosynthetic yield. Models like the one shown in Figure 1 quantify how specific changes in PSII physiology, such as in the estimates of σ and τ that can be determined using variable fluorescence techniques (PSII; Kolber and Falkowski 1992, 1993, Kolber et al. 1998), affect photosynthetic yields and rates in vivo. Yet target theory models as simple as these represent highly idealized representations of photosystem-photon interactions. They presumably omit important aspects of the physiology or organization of PSII that control the dynamics of photon capture and uptake. For example, a simple target theory model cannot account for the effect of pigment packaging (“self-shading”) on photosynthetic rates. Packaging is a common acclimative response to low light levels that involves changes to the layering of the thylakoid membranes (Berner et al. 1989), but application of target theory requires the assumption that all photosystems have an equal probability to absorb ambient photons. Pigment packaging inherently violates this assumption, as does any

physiological response in a plant or algal cell that causes some photosystems to shade others. A qualitatively similar response occurs under high-light conditions in those algae that move chloroplasts toward the nucleus as a strategy for photoacclimation (Furukawa et al. 1998). It might be possible to approximate such physiological responses analytically and embed these approximations into existing target theory models for the P - E relationship, but any resulting loss in realism may be difficult to quantify as would be any dynamical inaccuracies that such approximations introduce.

Recent studies suggest that dynamical aspects of the photosynthetic light reactions may be more important than previously thought. A range of feedback, threshold, and lagged behaviors have been identified (e.g., Nedbal and Březina 2002, Nedbal et al. 2003, Fragata and Dudekula 2005) that indicate strong nonlinear dynamics in light harvesting at the photosystem level. In other physiological systems, such behaviors are known to reflect important modes of regulation (Glass 2001, Strogatz 2001), and a reasonable hypothesis is that nonlinear dynamics at the photosystem level may introduce similarly important but as of yet unexamined effects on photosynthetic rates or yields. Models are powerful tools for identifying potential enhancements or regulations that arise from nonlinear dynamics, but modeling how nonlinear dynamics arise in light harvesting and quantifying their potential effect remains challenging. Most nonlinear systems are difficult or impossible to represent appropriately using equations (May 1976, Strogatz 1994, Glass 2001), and simple target theory models are not adequate for representing such nonlinear dynamics.

Many nonlinear systems can be well modeled using nonanalytical approaches (e.g., Lavorel 1986, Kevrekidis et al. 2004) including systems that can be thought of as a collection of targets, but where target theory does not adequately describe the system’s dynamics (e.g., Andreo 1991). To understand better how the dynamics of photon-photosystem interactions at the photosystem level may affect photon capture and light harvesting, a simple, intuitive non-analytical approach was developed to simulate how an idealized population of PSII interacts with a photon flux. This simulation can quantify the theoretical effect of changes in specific properties of individual PSII on rates and yields of light-driven electron flow, as well as the effect of population-wide changes such as the spatial density of PSII associated with pigment packaging or chloroplast movement within a cell. We applied this nonanalytical simulation in three different contexts to assess its utility for exploring basic dynamical aspects of light harvesting that cannot be readily modeled using equations. First, we quantified how specific changes in PSII structure, function, and organization would theoretically affect the dynamics of photon capture and light-driven electron flow in

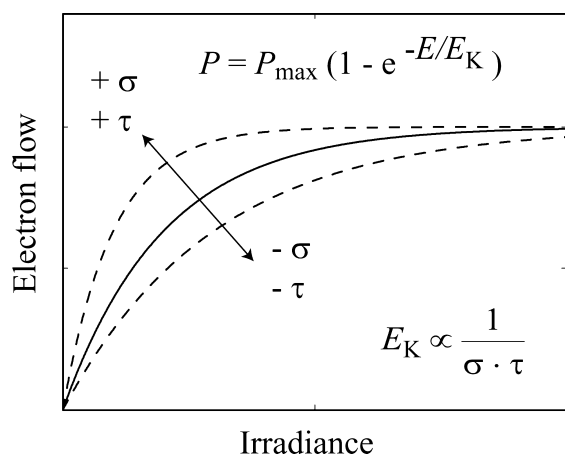


FIG. 1. A saturating relationship between irradiance (E) and photosynthesis (P) can be derived mechanistically from first principles using a target theory model of light-driven electron flow. Dashed lines indicate how 50% increases and decreases in the mean effective photosystem cross-section (σ) or the electron turnover timescale (τ) affect electron flow rate.

idealized PSII populations. Second, we used this simulation in an applied context to estimate how measured changes in the PSII properties of a phytoplankton culture would presumably affect its light-harvesting rates and yields. Third, we used this simulation as an exploratory tool to estimate how a basic nonlinear aspect of photosynthetic light harvesting, the transfer of absorbed photon energy among PSII (Falkowski et al. 1988), may introduce unpredicted enhancements or constraints on light-driven electron flow simply due to dynamical interactions among photosystems.

MATERIALS AND METHODS

Design of the simulation. PSII in this simulation are represented as circles, with a number of PSII (n_{PSII}) randomly distributed in a two-dimensional model domain of length scale L (Fig. 2). A given simulation run involves passing photons through this model space and assessing how this idealized PSII population absorbs and utilizes this photon flux. Before each run, every PSII is assigned a functional cross-section (σ_{PSII}) that describes its circular area and thus establishes its effective radius within the model space. A single time constant (τ_{PSII}) is used to represent the turnover timescale of the electron acceptors that service these PSII, which for simplicity is assumed to be identical for all PSII within the model domain. A fraction of these PSII can be considered nonfunctional photochemically to represent photodamage or other factors that affect PSII functionality. This fraction is represented by a term f_{PSII} where a value of 0.6 indicates that 60% of simulated

PSII are functional photochemically. The simulation also allows photon energy absorbed by one PSII to be transferred to another in a form of photosystem connectivity, which is parameterized by a probability of transfer (p) such that $p = 0$ represents a simple separate-units model (Bernhardt and Trissl 1999). The actual mechanism for this connectivity is not specified in this simulation, and no distinction is made between energy transfer at the thylakoid level (sensu Joliot and Joliot 1964) and transfer within cells via fluorescence emission and reabsorption (sensu Huot et al. 2005), although the latter in nature may be a less important source of energy transfer.

Once these properties are assigned to the PSII in a given population, PSII whose centers are located within one radius of the boundary of the model domain are repositioned back into the domain so that no part of any PSII is outside the domain. Next, the dynamical and steady-state behaviors of this population are determined at a particular irradiance, E , using a Monte Carlo method. Here, individual photons are passed sequentially through the model domain, and their energetic fates are recorded. The number of photon events to be simulated (n_{photons}) is computed from the simulated irradiance, E ; the area of the model domain, L^2 ; and the turnover timescale, τ_{PSII} .

$$n_{\text{photons}} = E \cdot L^2 \cdot 50\tau_{\text{PSII}} \cdot 10^{-3} \quad (2)$$

Running the simulation for a period 50 times longer than τ_{PSII} ensures that a dynamical equilibrium is reached and also helps to reduce statistical noise in the results. The factor of 10^{-3} converts the units of τ_{PSII} (ms) into seconds.

These n_{photons} are directed through the model domain randomly in space using the "ran1" algorithm of Press et al. (1992). The numerical period of this algorithm is greater than 10^8 , much larger than number of photons required to simulate the highest E in this study. Therefore, the locations of photons passing through the model domain are effectively randomized without repetition. Photons are passed through the model domain regularly in time, and although this is not strictly realistic, for simplicity, we ignored any effect that this difference would have over the relatively long timescales of a given simulation run.

The energetic fate of each of these n_{photons} photons is determined using a decision tree (Fig. 3). If a photon's randomly chosen coordinates in the model domain are located within the circular area of a particular PSII, this photon is considered to be absorbed by that PSII. If two or more PSII overlap this location, the PSII that was positioned first over those coordinates is considered to be the absorbing photosystem. The fate of an absorbed photon depends first on the immediate photochemical state of the PSII that absorbed it. If that PSII was designated as nonfunctional, the absorbed photon is considered to be dissipated as heat. If that PSII is photochemically functional, then its photochemical state is next evaluated. If it has not absorbed a photon within the prior $3\tau_{\text{PSII}}$, then that PSII is considered closed to photochemistry for a subsequent period of $3\tau_{\text{PSII}}$, and the absorbed photon counts toward photochemistry. For the purposes of this simulation, closure of a PSII is equivalent to the photochemical reduction in the associated primary quinone electron acceptor, Q_A , that occurs in actual organisms (Kolber et al. 1998, Samson et al. 1999), a definition often used in other modeling studies (e.g., Zhu et al. 2005). Photons absorbed by a closed PSII are considered to be dissipated via fluorescence, unless this photon energy is transferred to another PSII. Whether such transfer occurs for this particular photon is determined by a uniformly distributed random number generated between 0 and 1. If this number is less than p , this photon energy is redirected to another PSII randomly chosen within the model domain.

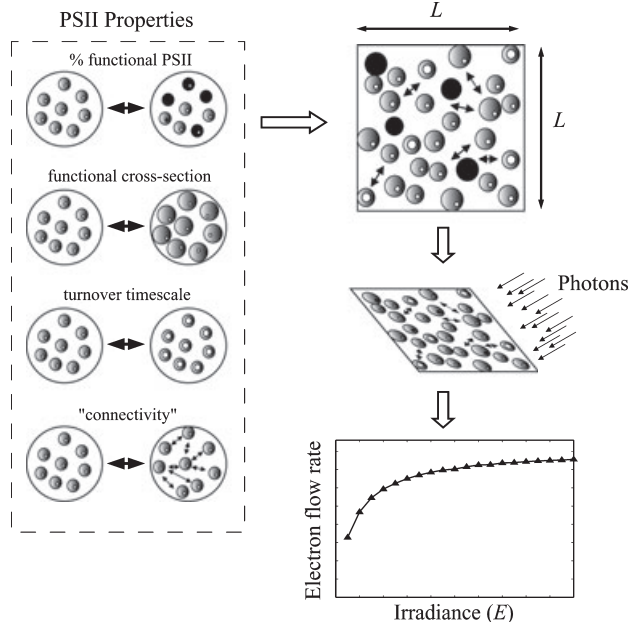


FIG. 2. This simulation models a number of PSII with specified photosynthetic properties, distributed in a model domain of area L^2 . A photon flux representing an irradiance (E) is randomly directed through L^2 , and a relative rate of light-driven electron flow (P_e) is computed from the number of photons that encounter open, functional PSII. By simulating electron flow rates over a range of different E -values, it is possible to generate the P_e - E relationship of a particular population of modeled PSII for that specific combination of photosynthetic properties.

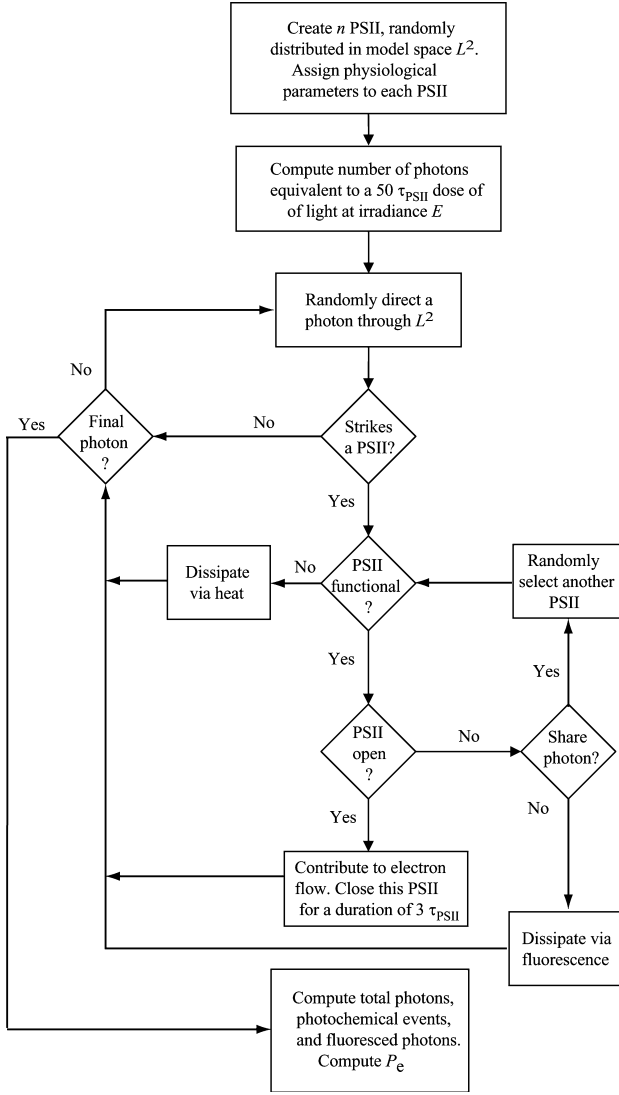


FIG. 3. The decision tree used to represent the photon-photosystem dynamics in this simulation. The photosynthetic properties of the photosystems and their location in the model domain are first specified, after which a Monte Carlo method is used to repeatedly track the energetic fates of individual photons passing through this model domain.

After the last of these n_{photons} is either dissipated or counted toward photochemistry, the total number of photons that closed PSII and therefore contributed to light-driven electron flow ($n_{\text{electronflow}}$) is computed. The number of fluoresced photons ($n_{\text{fluoresced}}$) is also calculated. A steady-state rate of electron flow P_e (electrons \cdot s $^{-1}$) is calculated by normalizing the number of photons that closed a PSII in a given simulation run to the run's duration in model time ($50\tau_{\text{PSII}}$, in ms).

$$P_e = \frac{n_{\text{electronflow}}}{50\tau_{\text{PSII}} \cdot 10^{-3}} \quad (3)$$

The factor of 10^{-3} again converts the units of ms into s. These electron flow rates have no meaning in an absolute sense, but relative changes in P_e indicate the effect of different PSII properties or architectures. The yield of electron flow (Φ^P) is computed as

$$\Phi^P = \frac{n_{\text{electronflow}}}{n_{\text{photons}}} \quad (4)$$

and the steady-state yield of fluorescence emission (Φ^F) is similarly computed as

$$\Phi^F = \frac{n_{\text{fluoresced}}}{n_{\text{photons}}} \quad (5)$$

These yields are normalized to the number of photons directed through the model domain, not to the number of photons absorbed by PSII. The sum of Φ^F and Φ^P is not unity because of the pathway for dissipation via heat.

This simulation does not explicitly include any allowance for dynamical changes in processes like nonphotochemical quenching of fluorescence. For simplicity, such processes are assumed to be constant over the short $50\tau_{\text{PSII}}$ timescale of any given simulation run. Similarly, the efficiency with which absorbed energy is transferred to reaction centers in PSII is also not represented in the simulation nor is the quantum yield of charge separation. Terms for these sometimes appear in analytical equations for light-driven electron flow (Table 1) but are often defined as unity and included for heuristic purposes only, not as model parameters per se.

The length scale of the model domain (L) was selected so that P_e saturated at roughly the same E that is observed in actual phytoplankton (i.e., on the order of $100 \mu\text{mol quanta} \cdot \text{m}^{-2} \cdot \text{s}^{-1}$ for typical values of σ_{PSII} , τ_{PSII} , and f_{PSII}). This tuning of L introduces no bias in the simulated light-harvesting dynamics, provided that excessive self-shading of PSII is avoided. An additional benefit of adjusting L in this way is that physiologically realistic values of σ_{PSII} , τ_{PSII} , f_{PSII} , and p can be used in the simulation, making it unnecessary to scale these parameters as well.

Assessing steady-state and transient dynamics of the simulation. The P_e - E relationship of a particular PSII population can be generated by repeatedly simulating P_e over a range of different irradiances. We determined the P_e - E relationships of a wide but physiologically realistic range of PSII populations, which represented the different combinations of σ_{PSII} , τ_{PSII} , p , and

TABLE 1. Some published equations for computing light-driven electron flow from E and from physiological properties of PSII. Notation is not standardized: generally, variants of P refer to an electron flow rate, variants of σ refer to a functional absorption cross-section, and I or E is irradiance. Variants of $\Delta\phi$ represent photochemical yields, and Φ and q refer to efficiencies. Both n_{PSII} and n_{PS2} represent the number of PSII.

Model equation	Reference
$P = n \cdot \sigma_{\text{PSII}} \cdot \phi \cdot I$	Sukenik et al. 1987 (eq. 1)
$P = I \cdot \sigma_{\text{PSII}} \cdot \Phi_q \cdot \Phi_t \cdot \Delta\phi_{\text{sat}}$	Kolber and Falkowski 1992 (eq. 1)
$P_f = \left[\frac{\Delta\phi_p}{0.65} \right] \cdot q_p \cdot E \cdot \sigma_{\text{PSII}}$	Falkowski and Kolber 1993 (eq. 5)
$P_{O_2}^B(E) = \sigma_{\text{PS2}} \cdot \Phi_{RC} \cdot q_P(E) \cdot \phi_e(E) \cdot f \cdot n_{\text{PS2}} \cdot E$	Kolber and Falkowski 1993 (eq. 12)
$P = I \cdot \sigma_{\text{PSII}} \cdot n_{\text{PSII}} \cdot qP \cdot \left[\frac{\phi_{\text{sat}}}{1.7} \right]$	Falkowski and Kolber 1995 (eq. 4)
$P_f = E \cdot \sigma_{\text{PSII}} \cdot \frac{\Delta F'}{F'}$	Falkowski and Kolber 1995 (eq. 9)
$P^{RCII}(E) = E \cdot \sigma_{\text{PSII}} \cdot qP(E) \cdot \phi_e(E) \cdot f$	Gorbunov et al. 2000 (eq. 1)
	Suggett et al. 2001 (eq. 1)

TABLE 2. The ranges of PSII properties and irradiance examined in this simulation.

Parameter	Simulated values	Units
n_{PSII}	250	dimensionless
L	$0.5 \cdot 10^{-7}$ (50) or $1 \cdot 10^{-7}$ (100)	m (nm)
E	0.1, 0.2, ... 50, 60, ... 200, 250 ... 500	$\mu\text{mol quanta} \cdot \text{m}^{-2} \cdot \text{s}^{-1}$
σ_{PSII}	200, 300, ... 1,200	$\text{\AA}^2 \cdot \text{quanta}^{-1} \cdot \text{PSII}^{-1}$
p	0, 0.05, ... 0.5	dimensionless
τ_{PSII}	1, 2, ... 10	ms
f_{PSII}	0.05, 0.1, ... 0.65	dimensionless

f_{PSII} shown in Table 2. Increments of simulated E were spaced unevenly to provide fine resolution at low E and progressively coarser resolution at higher E . Two replicate sets of simulation runs were performed over these ranges to examine how differences in the spatial density of PSII, such as that resulting from changes in pigment packaging or chloroplast migration, may affect light harvesting. The first used 250 PSII in a model domain of $L = 50$ nm, resulting in a PSII population that was “densely” distributed with overlap that was significant but not extreme (Fig. 4a). The second used the same number of PSII in a model domain with $L = 100$ nm, resulting in a more “sparsely” distributed PSII population with minimal overlap (Fig. 4b). Although such “dense” PSII populations would often be associated with low-light photoacclimation, such as pigment packaging and self-shading, PSII will be to some degree similarly self-shaded in a cell that has responded to high-light conditions by moving chloroplasts toward the nucleus (Furukawa et al. 1998). Modeling photon-photosystem interactions in both “dense” and “sparse” PSII populations provides a means to examine how PSII overlap within a cell affects its P - E relationship in the most general sense, not just in the manner traditionally associated with low-light acclimation and thylakoid-level pigment packaging, which would likely coincide with only a limited subset of the PSII property combinations listed in Table 2.

RESULTS

Dynamical and steady-state behavior of the simulation. Examining the step response of this simulation is

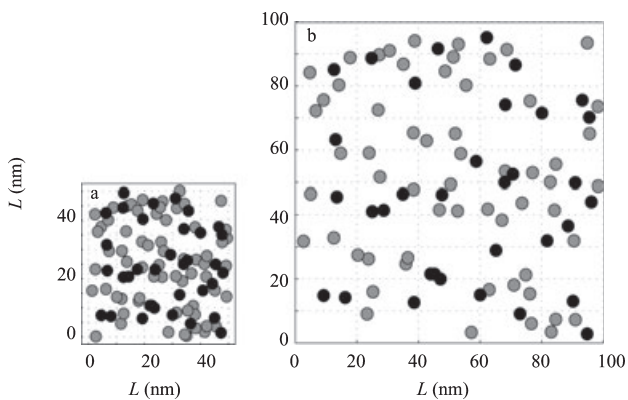


FIG. 4. Two example PSII populations having the same n_{PSII} but (a) with some degree of overlap among PSII ($L = 50$ nm), to simulate pigment packaging or PSII overlap, and (b) with minimal packaging or overlap ($L = 100$ nm). The PSII in these two examples are scaled appropriately to indicate their relative size compared to the model domain.

one way to evaluate how accurately it replicates photon capture and uptake dynamics. When dark-adapted plants and algae experience a high-intensity step increase in irradiance, virtually all PSII rapidly close due to reduction in the primary electron acceptor, Q_A . Given adequate intensities, this action can result in a transient rise in variable fluorescence on the sub-ms timescale (Kolber et al. 1998, Samson et al. 1999, Kromkamp and Forster 2003). This timescale is much shorter than that of a single photochemical turnover, and so this fluorescence transient is often referred to as the “photochemical” phase of fluorescence induction (Samson et al. 1999). The fluorescence maximum attained on these scales is variously referred to as J , I_1 , F_m , or $F_{m(\text{ST})}$ in the literature (Strasser et al. 1995, Kromkamp and Forster 2003), and for notational convenience, we will refer to this level heretofore as F_m . A model of light harvesting that is dynamically realistic on this timescale should be able to reproduce this transient rise in fluorescence to F_m as well as this full closure of PSII.

Both of these dynamical behaviors can be seen in the output of this nonanalytical simulation during the first 100 μs of a simulated run at very high E ($20,000 \mu\text{mol quanta} \cdot \text{m}^{-2} \cdot \text{s}^{-1}$, Fig. 5). To examine these transients more clearly over these short model timescales ($\ll \tau_{\text{PSII}}$), it was necessary to use a larger model domain ($L = 4e-7$ m) and a greater number of PSII ($n_{\text{PSII}} = 4,000$) to reduce nonanalytical noise. On these timescales, f_{PSII} is an appropriate proxy for the variable fluorescence yield F_v/F_m described by the Kolber et al. (1998) physiological model of variable fluorescence, where F_m is defined as above. The variable fluorescence kinetics produced by this simulation were well fit by the Kolber et al. model, with fitted estimates of σ_{PSII} and f_{PSII} (F_v/F_m) within 2.5% and 12% of the values assigned to them for this particular simulation run. The number of open PSII decreased to zero during this period, indicating that this fluorescence behavior coincided with complete photochemical closure of the entire PSII population, as would be expected to occur on such timescales due to the complete reduction in Q_A at such high irradiance levels. It should be noted that experimentally measured fluorescence transients may be faster or slower than the simulated one in Figure 5, but that this discrepancy does not indicate that the simulation is dynamically inaccurate. In reality, a given PSII population can exhibit a wide range of timescales in this photochemical phase fluorescence transient simply due to the intensity of the light source used to stimulate fluorescence. Bright sources will result in faster saturation and PSII closure than dimmer sources, and these same dynamics can be observed in this simulation.

The shape of the steady-state P_e - E relationships predicted by the simulation further suggested that it reproduced realistic dynamics in light harvesting.

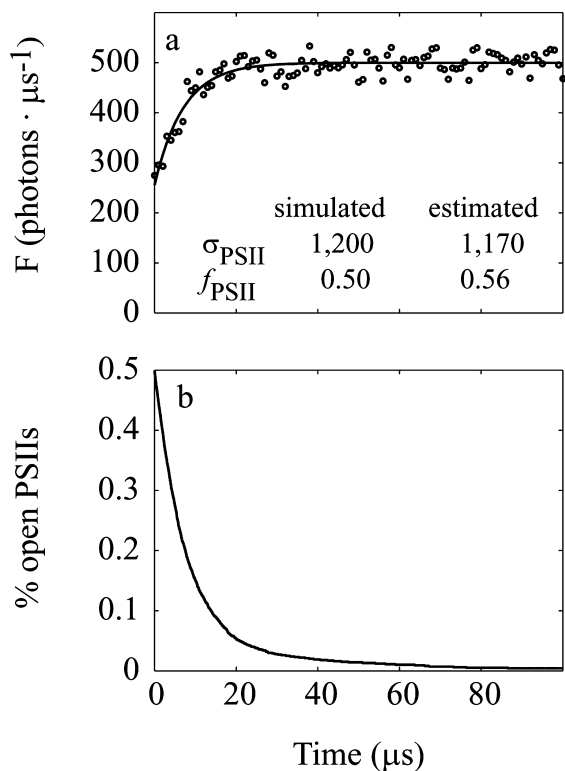


FIG. 5. The simulated step response of a low spatial density ($L = 400$ nm) population of PSII ($n_{\text{PSII}} = 4,000$) to a strong step increase in E from 0 to $20,000 \mu\text{mol quanta} \cdot \text{m}^{-2} \cdot \text{s}^{-1}$. A fit of a theoretical model for fluorescence yield kinetics (a) produced estimates of σ_{PSII} and f_{PSII} similar to those used to generate this transient. The fraction of open PSII (b) decreased from the initial f_{PSII} of 0.5 to zero during this transient, indicating complete photochemical closure of this PSII population. In this situation, the variable fluorescence yield F_v/F_m measured from actual transients was considered equivalent to f_{PSII} .

We observed that for a simple PSII population with minimal overlap and no energy transfer between PSII, the P_e - E relationship of this population was best fit by a rectangular hyperbola (Fig. 6a). Other functional forms for P - E (see Table 3) did not fit as well, or they required additional “shape” parameters whose best-fit estimates effectively reduced them all to rectangular hyperbolae. The PSII population we used for this initial examination (i.e., minimal overlap, $p = 0$) is simple enough so that its energetic dynamics can be represented analytically with differential equations whose solution is a hyperbola (Han 2001). Good agreement between theory and simulation with this simple case provides assurance that the simulation will reproduce realistic dynamics when modeling more complex PSII architectures whose dynamics may not have an analytical solution.

A simple sensitivity study with this simple PSII population demonstrated how independent changes in these PSII properties each affected overall electron flow rates. Independent decreases in either f_{PSII} (Fig. 6b, + symbols) or σ_{PSII} (Δ sym-

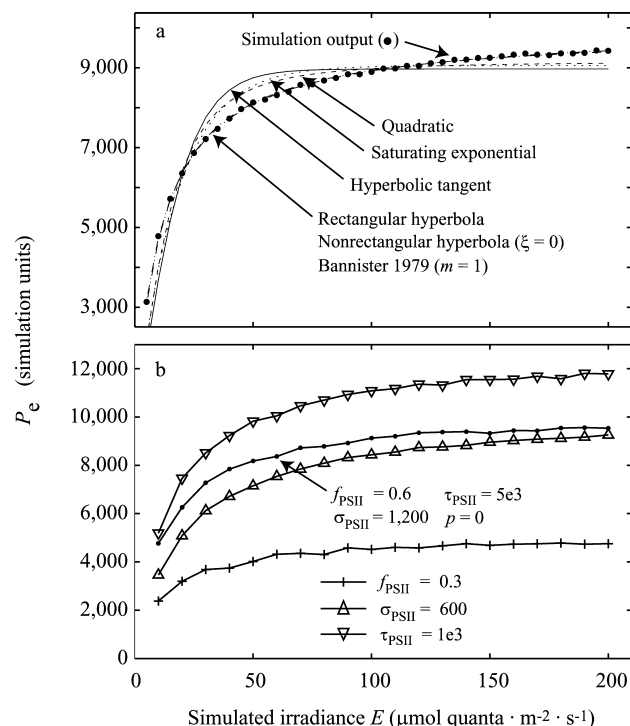


FIG. 6. (a) Fits of six different functional forms for P - E to a P_e - E relationship simulated from a simple PSII population. A simple hyperbola provides the best fit with the fewest parameters. (b) Examples of P_e - E relationships predicted for the same population showing how independent changes to f_{PSII} , σ_{PSII} , τ_{PSII} , and p each affect the simulated electron flow rate in that particular population.

both resulted in decreases in steady-state P_e . This change was expected because decreased numbers of functional PSII and smaller functional cross-sections each act to reduce electron flow. Shortening τ_{PSII} (∇ symbols) led to an increase in steady-state P_e , a response that reflects a fundamental difference between how τ_{PSII} acts in this dynamical simulation and how τ acts in the quasi-mechanistic model of Figure 1. Small changes in τ in the model of Figure 1 primarily affect E_K only and not the steady-state P_e , whereas in this dynamical model, changes in τ_{PSII} do affect P_e because they alter the effective energy throughput for all PSII.

These P_e - E relationships do not exhibit any reduction in electron flow at very high E , that is, the “photoinhibition” often seen in nature that is sometimes represented in empirical P - E models by the β parameter (Platt et al. 1980). This apparent lack of photoinhibition is to be expected, because these P_e - E relationships arise from PSII populations the physiological properties of which are fixed. Without changes in physiology, a PSII population can only be undersaturated or effectively saturated at any given photon flux, and so there should be no expectation that P_e decreases at supraoptimal E in this model.

TABLE 3. Functional forms of P - E fitted to the simulated P_e - E relationships. Similar equations may substitute E_K for $P_{\max} \cdot \alpha^{-1}$, or I for E . The m in Bannister (1979) and ξ in Thornley (1998) are shape parameters that reduce these equations to simple hyperbolae when $m = 1$ or when $\xi = 0$.

$P(E) = \frac{\alpha E P_{\max}}{(\alpha E + P_{\max})}$	Rectangular hyperbola (Maskell 1928, Baly 1935)
$\frac{P_{\max} \alpha E}{\sqrt{P_{\max}^2 + (\alpha E)^2}}$	Quadratic (Smith 1936)
$\frac{v_m I}{(I_p^m + I^m)^{\frac{1}{m}}}$	Generalized empirical form (Bannister 1979)
$P_{\max} \left(1 - e^{-\frac{\alpha E}{P_{\max}}}\right)$	Saturating exponential (Webb et al. 1974)
$P_{\max} \tanh\left(\frac{\alpha E}{P_{\max}}\right)$	Hyperbolic tangent (Jassby and Platt 1976)
$\frac{1}{2\xi} \left[\alpha E + P_{\max} - \sqrt{(\alpha E + P_{\max})^2 - 4\xi \alpha E P_{\max}} \right]$	Nonrectangular hyperbola (Thornley 1998)

Potential enhancement in electron flow due to PSII energy transfer. The P_e -values that were computed from these simulation runs indicated that the transfer of absorbed photon energy between PSII could have a strong nonlinear effect on light-harvesting rates and yields. In two representative runs, PSII populations with a p of 0.5 exhibited an enhancement in P_e by $\approx 8\%$ to 10% compared to populations that were identical in all respects except for having no energetic connectivity (Fig. 7a). In these two cases, the enhancement was higher in the PSII population that saturated at lower E (Fig. 7b), and in both populations, this enhancement was maximal at irradiances below the “dynamical” E_K that would be predicted from the population’s σ_{PSII} and τ_{PSII} using equation 1 (arrows). In neither case did this enhancement decrease to zero at irradiances that

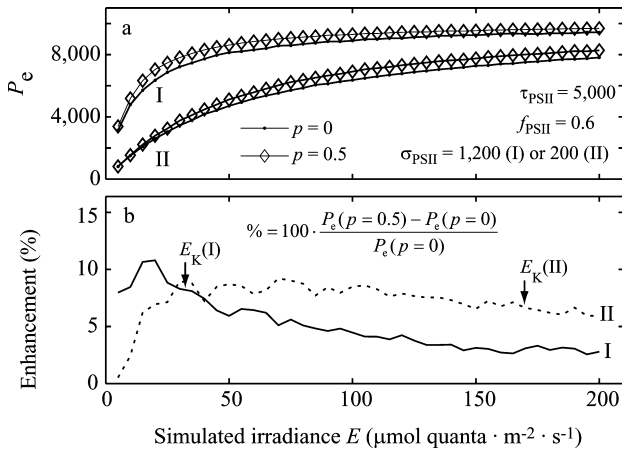


FIG. 7. Enhancement in P_e over a range of E values due to energy transfer between PSII. In (a), two specific PSII physiological states are shown (I and II), the former having a larger functional cross-section and therefore exhibiting saturation in P_e at a lower E . Having a p of 0.5 (diamonds) compared to one of zero (dots) results in an up to 10% enhancement in P_e (b), with the greatest enhancement occurring at irradiances lower than would be predicted by computing the “dynamical” E_K from equation 1 (arrows).

would typically be considered light saturating, remaining instead $\approx 3\%$ to 6% .

More complex differences in p -driven enhancement of P_e occurred in the simulations run over the broader physiological ranges of σ_{PSII} , τ_{PSII} , p , f_{PSII} , and E in Table 2. To concentrate on the more

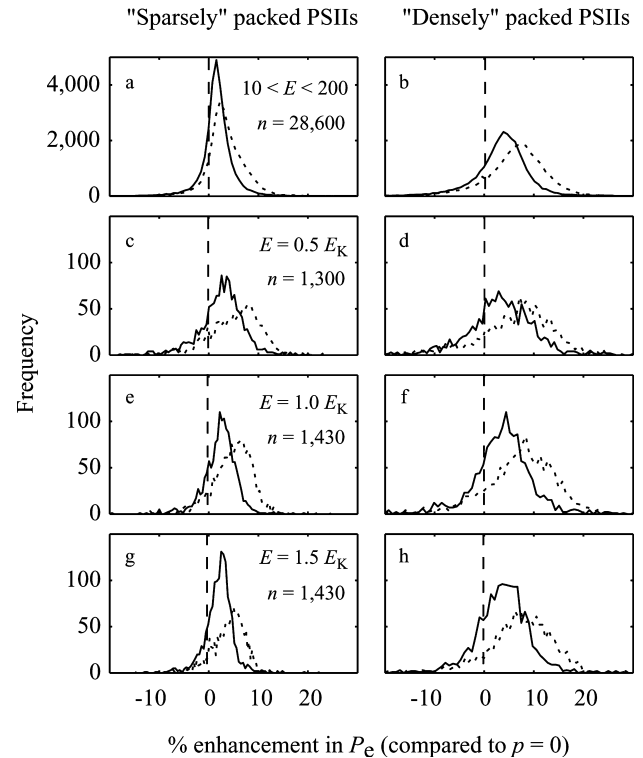


FIG. 8. Percent enhancement of P_e due to energy transfer between PSII for a model domain that is sparsely populated with PSII (left column, i.e., Fig. 3b) and one that is densely populated (right column, i.e., Fig. 3a). Solid lines show results for $p = 0.25$ and dotted lines for $p = 0.5$. Histograms in the top row include all P_e - E curves simulated between 10 and $200 \mu\text{mol quanta} \cdot \text{m}^{-2} \cdot \text{s}^{-1}$. The bottom three rows show subsets of these curves at specific irradiances relative to E_K : $E = 1.0 E_K$ (row 2), $E = 0.5 E_K$ (row 3), and $E = 1.5 E_K$ (row 4).

ecologically relevant range of E around E_K , we examined this enhancement only in those simulations with $10 < E < 200 \mu\text{mol quanta} \cdot \text{m}^{-2} \cdot \text{s}^{-1}$. We determined that the level of enhancement in P_e differed in these 28,600 simulations between the “sparse” and “dense” PSII populations. In a sparse PSII population, the enhancement due to $p = 0.25$ was distributed in a roughly Gaussian fashion $\approx 2\%$ (Fig. 8a, solid trace). The positive tail of this distribution indicated enhancement in excess of 10% for certain combinations of σ_{PSII} , τ_{PSII} , and f_{PSII} . The negative tail indicated that nonzero energy transfer between PSII could actually act to decrease P_e given other combinations of these PSII properties. Doubling the degree of energy transfer ($p = 0.5$, dashed trace) resulted in a broader distribution with a peak located slightly higher at $\approx 3\%$. In dense PSII populations, this p -driven enhancement was stronger and more broadly distributed, $\approx 4\%$ and 9% for $p = 0.25$ and 0.5 , respectively (Fig. 8b). The tails of these distributions indicated a potential enhancement in P_e of up to 20% for certain physiological combinations, and a reduction by $\approx 15\%$ for others.

These summary histograms contain information on how this p -driven enhancement depends on various combinations of the four specified PSII physiological properties, but this multidimensional variability is difficult to interpret in such summaries. To explore this better, we used equation 1 to compute the photosystem-level E_K for each of these 28,600 simulated PSII populations from its specified σ_{PSII} and τ_{PSII} . We selected from these populations only those runs that fit into one of the following three categories: (i) runs where E was half of this computed E_K , (ii) runs where E was equal to E_K , and (iii) runs where E was 1.5 times greater than E_K . These categories correspond to PSII populations that in theory are either dynamically undersaturated by, equilibrated to, or oversaturated by the ambient photon flux. We observed that in sparsely distributed PSII populations, the enhancement in P_e due to energy transfer decreased as E surpassed E_K (e.g., for $p = 0.25$ in Fig. 8c, e, and g, solid lines). This effect was more evident in a similar PSII population with twice the degree of energy transfer ($p = 0.5$, dashed lines). In dense populations, the enhancement in P_e was less sensitive to the relationship between ambient E and E_K (Fig. 8, d, f, and h), although in general it displayed a broader distribution.

Using this simulation to interpret measured time series of PSII variability. Repeated simulation of P_e over the ranges of PSII properties in Table 2 effectively generates a look-up table of P_e at specific combinations of σ_{PSII} , τ_{PSII} , p , f_{PSII} , and E . Because our definitions for these parameters are roughly analogous to those used by experimentalists, this table provides a means to predict how measured changes in σ_{PSII} , τ_{PSII} , f_{PSII} , and p in actual phytoplankton may affect their light-driven electron flow rates. We used this approach to predict relative changes in P_e in a

nutrient-limited culture of *Thalassiosira weissflogii*, the PSII physiological properties of which were continuously measured using fast repetition rate (FRR) fluorometry (see Laney et al. 2005). This variable fluorescence technique can generate highly resolved time series of proxies for σ_{PSII} , τ_{PSII} , and p , but it does not provide direct measurements of f_{PSII} (Kolber et al. 1998). For this assessment, we used the variable fluorescence yield F_v/F_m as a proxy for f_{PSII} , realizing that changes in this yield often, but not always, reflect changes to the fraction of functional PSII (Falkowski and Kolber 1995, Parkhill et al. 2001). To correct better for measurement biases, variable fluorescence data from the 2005 study were first reprocessed using a more recent improved approach (Laney and Letelier 2008).

Considerable variability was observed in the measured PSII properties in this culture, presumably reflecting diurnal cycles as well as longer-term responses to a deliberate increase in E that occurred halfway through this study (Fig. 9). Despite such independent variability in specific PSII parameters, the overall P_e - E relationships predicted by the simulation were similar to those expected for algae

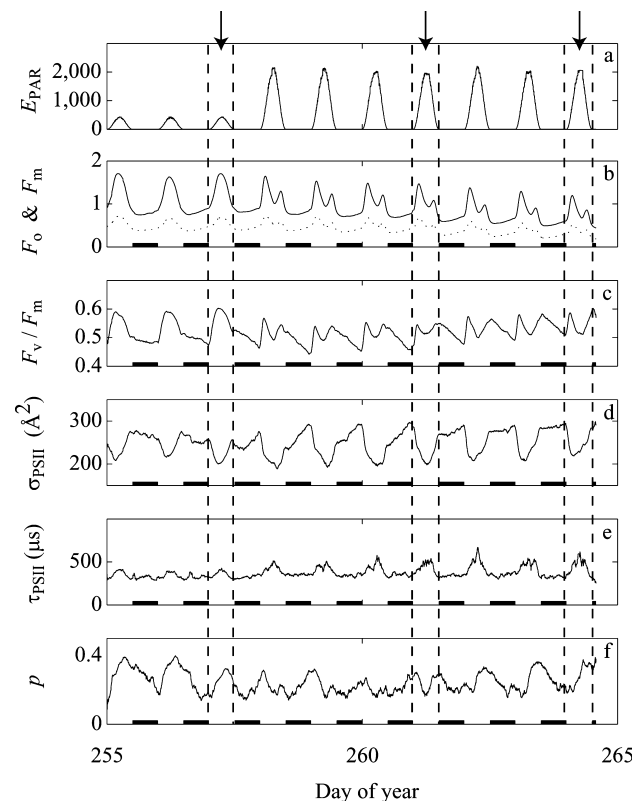


FIG. 9. Photosynthetically active growth irradiance (PAR, a) and PSII physiological properties (b–f) measured in a 10 d culture of *Thalassiosira weissflogii* (for experiment details refer to Laney et al. 2005). Arrows and vertical dashed lines indicate 3 specific days that were examined with this simulation to predict relative changes in P_e (see Fig. 10). Thick bars on the abscissa indicate periods in (a) when the growth lamps were off.

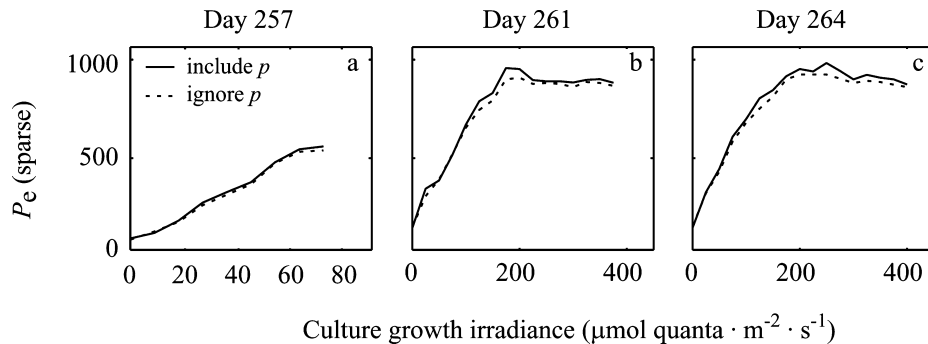


FIG. 10. Predicted P_e - E relationships for the forenoon of the 3 d indicated in Figure 9: (a) acclimated to low light, low nitrate conditions; (b) transiently acclimating to higher E ; and (c) further acclimated to high E . Solid lines represent P_e - E relationships when all physiological parameters were included. Dashed lines indicate simulations where the effect of PSII connectivity was ignored and p was fixed to 0. The enhancement in P_e is most evident in these curves around the irradiance that would correspond to E_K in an empirical P - E curve.

under low- and high-light conditions. On a day early in the time series when the culture was acclimated to low light levels, the P_e - E relationship displayed a generally linear trend in the morning period (Fig. 10a, solid lines). This linear relationship was maintained despite considerable physiological variability in PSII during this several-hour period (see day 257 in Fig. 9, a-e). Four days later, after a shift to higher E , this linear relationship became more like what is expected of light-saturated cells (Fig. 10b), with a slight midday reduction in P_e also apparent. The P_e - E relationship 3 d later continued to exhibit this same saturating behavior (Fig. 10c), although its shape had changed slightly. Unlike the P_e - E relationships generated from “static” PSII population (e.g., Fig. 7), the relationships generated from actual time series of PSII physiology do exhibit a reduction in P_e at high E . This finding indicates that PSII physiology in these cultures changes during the day as the cells acclimate, experience photo-damage, or are otherwise altered by being exposed to high irradiance around solar noon. These changes affect the shape of these P_e - E curves and lead them to differ from those exhibited by populations with fixed PSII physiology.

Using these same experimental observations, we examined the degree to which these predicted P_e -values would differ due to the effect of energy transfer between PSII. We recreated a duplicate time series of P_e using our look-up table as before, but by fixing p at 0 regardless of its actual measured value. We then calculated the percent difference between these predicted P_e -values and those predicted using the p that was actually measured. Ignoring PSII energy transfer in this simulation resulted in estimates of P_e that were smaller by $\approx 5\%$ - 10% in both sparsely and densely modeled populations of PSII (Fig. 10, dashed lines) for this particular time series of PSII properties. The enhancement in P_e due to connectivity was most pronounced in the region immediately around the irradiance that would represent E_K in empirical P - E models.

DISCUSSION

Simulating light-harvesting dynamics among PSII. Experimental techniques such as variable fluorescence analysis have provided valuable insight into how aspects of PSII physiology affect photosynthetic rates and yields. This insight is limited, however, because only a few aspects of PSII physiology can be reliably measured in laboratory cultures and even fewer in natural assemblages. Despite this fact, models have been developed to interpret this incomplete view of PSII physiological variability in phytoplankton in metabolically and ecologically meaningful terms. Equations that estimate how measured changes in PSII physiology should affect light-driven electron flow rates (e.g., Table 1) are in essence PSII-based equations for the P_e - E relationship. Such equations have the potential to assess the general photosynthetic state of phytoplankton directly from PSII properties, yet it is unclear how accurately these equations are in modeling the physiological control of PSII on light harvesting. Improving PSII-based models for light harvesting involves not only identifying aspects of photosynthetic physiology that are currently missing, but also identifying ways in which the real relationship between PSII physiology and P_e might not be accurately represented. An important criterion for these models is whether they are dynamically realistic in their descriptions of photon capture and uptake.

The equations in Table 1 are dynamically linear because changes in a particular property of a PSII population, such as the PSII functional cross-section, have a direct and proportional effect on photosynthetic rates and yields. Recent studies, however, suggest that the photosynthetic light reactions are not so clearly linear in this manner but rather can exhibit strong nonlinear dynamics (Nedbal and Březina 2002, Nedbal et al. 2003, Fragata and Dudekula 2005, Rascher and Nedbal 2006). If the capture and uptake of photons at the photosystem level is sufficiently nonlinear in a dynamical sense, then small changes in a particular PSII property

may actually have a disproportionately strong effect on light-harvesting rates or yields, which would not occur in a dynamically linear system. Nonlinear dynamics are now known to play important regulatory roles in many physiological systems (Korn 2005), and a reasonable hypothesis is that they also play an important role in regulating photosynthesis in plants and algae. Analytical models will probably not help us identify nonlinear dynamics in the P_e - E relationship because many nonlinear systems cannot be represented accurately using equations (May 1976, Strogatz 1994). Even in instances where it may be possible to approximate a particular nonlinear behavior analytically, it can be difficult to identify or quantify any dynamical artifacts that might result from such an approximation.

Nonanalytical approaches such as agent-based modeling and kinetic Monte Carlo simulation have proved useful for modeling the dynamics of nonlinear systems and for identifying nonlinear interactions within them (Kevrekidis et al. 2004). We used such an approach to replicate physiologically realistic steady-state and transient behaviors in PSII closure and fluorescence, using only a simple decision tree and Monte Carlo techniques (Fig. 5). The simulated dynamics of a simple PSII population that had an equivalent analytical representation matched closely those of the analytical solution, indicating that the design of the simulation was dynamically accurate (Fig. 6a). This is strong evidence that any nonlinear behavior that is observed in slight variations on this basic PSII population is also likely to be dynamically realistic and not simply numerical artifact resulting from improper simulation design or execution.

A nonanalytical approach is particularly valuable for examining a number of physiological changes in PSII the dynamical effects of which cannot be readily described using analytical equations. An example is with phytoplankton the PSII's of which are self-shaded at the thylakoid level due to pigment packaging or otherwise shielded due to the spatial arrangement of chloroplasts within the cell. Equations of basic target theory typically require an a priori assumption that all PSII's have an equal probability to absorb ambient photons. Yet with self-shading in actual cells, this assumption is inappropriate. A nonanalytical approach can directly express and quantify the dilatory effect of self-shading on PSII electron flow rates and yields, and it can also estimate the mitigating effect that processes like energetic connectivity among PSII's could potentially have in such situations. PSII connectivity can in theory redistribute absorbed photon energy among the entire PSII population and deliver exciton energy to PSII's that do not directly absorb a photon. Our simulations suggest that this mitigating enhancement effect can be substantial, exceeding 20%, given certain combinations of σ_{PSII} , τ_{PSII} , and f_{PSII} .

This mitigating effect of PSII connectivity on light harvesting is not a new idea, yet quantitative estimates of this effect have remained elusive. Because it is a nonlinear effect, it cannot be assumed that this connectivity-driven enhancement of P_e would exhibit a simple distribution in the parameter space of σ_{PSII} , τ_{PSII} , and f_{PSII} . Our results indicated that connectivity-driven enhancement not only was strongly skewed (Fig. 8), but that the same process could also act to constrain P_e in PSII populations with certain physiological combinations of properties, that is, those associated with the negative tails of these distributions. To the best of our knowledge, a potential for connectivity-driven constraint of P_e has not before been suggested, yet our simulation demonstrates that it arises from the same physiological mechanism that generates enhancements in P_e . These complex and counteracting nonlinear effects would be difficult to predict using analytical models, yet they can be computed straightforwardly with such a nonanalytical approach.

Apparent changes in the measured connectivity parameter p that are observed in cultures and in nature (e.g., Fig. 9f) presumably reflect alteration to PSII connectivity and not artifact (Laney 2003). Future experimental studies to assess these observed changes in actual phytoplankton, among different taxa and under realistic growth conditions, may consider examining not only its potential enhancing effect on P_e , but also the possibility that it may act to constrain P_e under other photosynthetic states. A wide range of similarly complex aspects of PSII populations can also be examined using a nonanalytical approach like ours, simply by modifying the simulation's decision tree and model domain. How the P_e - E relationship is affected by changes in photosystem stoichiometry and organization (Kim et al. 1993), different modes of photoprotective response (e.g., Lavaud et al. 2004), heterogeneity among PSII's (Kaftan et al. 1999), differences in antenna organization (Bernhardt and Trissl 1999), spectral variability in light utilization (Falkowski and LaRoche 1991), or the potential role for reabsorption of PSII fluorescence by PSI can all be examined using this type of nonanalytical simulation. Nonanalytical approaches were computationally prohibitive in the past, but the affordability of calculations on modern computers allows for inexpensive and quick simulation of complex PSII dynamics. We did not attempt to optimize for computational efficiency in our preliminary study, but used simple methods to keep the simulation clear and intuitive. Future simulations can take advantage of computational methods that improve the speed and efficiency without losing dynamical accuracy.

Some caveats and concerns. This simulation was developed primarily as an exploratory tool to identify and quantify how changes in PSII physiology could introduce complex nonlinear dynamics in light harvesting in a PSII population. It need

not be predictive in a traditional sense to be valuable; guiding development of testable hypotheses and providing theoretical motivations for experimental studies are appropriate uses of such simulations (e.g., Franks 2002). This approach does have several limitations, however, that merit discussion.

By focusing on the dynamics of PSII alone and omitting other aspects of the light reactions, such as PSI and the electron transport chain, we have effectively restricted the types of dynamics that this simulation can replicate. For example, the simulation performs reasonably well in predicting the dynamics of PSII closure and variable fluorescence during the sub-ms photochemical phase, but it cannot reproduce any of the fluorescence transients that are known to occur in the subsequent several ms in the thermal phase. Whether the simulation's dynamical predictions can still be considered valid despite omitting PSI and other important elements of the light reactions depends to a large extent on how these different elements are related to one another dynamically. It does not appear at present that these later thermal phase transients are associated with closure of PSII (Strasser et al. 1995, Samson et al. 1999), and thus we assume that the physiological bases of thermal phase fluorescence transients do not affect any of basic aspects of the simulation (e.g., n_{PSII} , σ_{PSII} , τ_{PSII} , β , f_{PSII} , the structure of the model domain, or the decision tree). If so, we can expect that the predicted dynamics of PSII closure and fluorescence should be independent of the thermal phase. In this case, incorporating additional aspects of the light reactions would not improve or affect the light-harvesting dynamics that the simulation predicts.

A number of recent analytical models do explicitly include other major components of the light reactions (e.g., Nedbal et al. 2005, Zhu et al. 2005, Kroon and Thoms 2006), and PSII-specific simulations like ours are important complements to these more complex models. Processes that are only parameterized in the former are explicitly defined in the latter, and vice versa. One limitation with these more complex models is that they remain difficult to apply in an ecological context because a more complete description of the light reactions requires numerous parameters that are either difficult or impossible to measure experimentally. Simpler PSII-based P_e - E models may be advantageous because they estimate relative changes in P_e from observed variability in a small number of measurable PSII properties. Yet when applying these simpler models in this manner, special care must be taken to ensure that the measured PSII properties used as input are appropriate proxies for the idealized PSII properties as defined in the model. For example, when we used this simulation to interpret measured changes in PSII from a *T. weissflogii* culture, we made the simplifying assumption that F_v/F_m

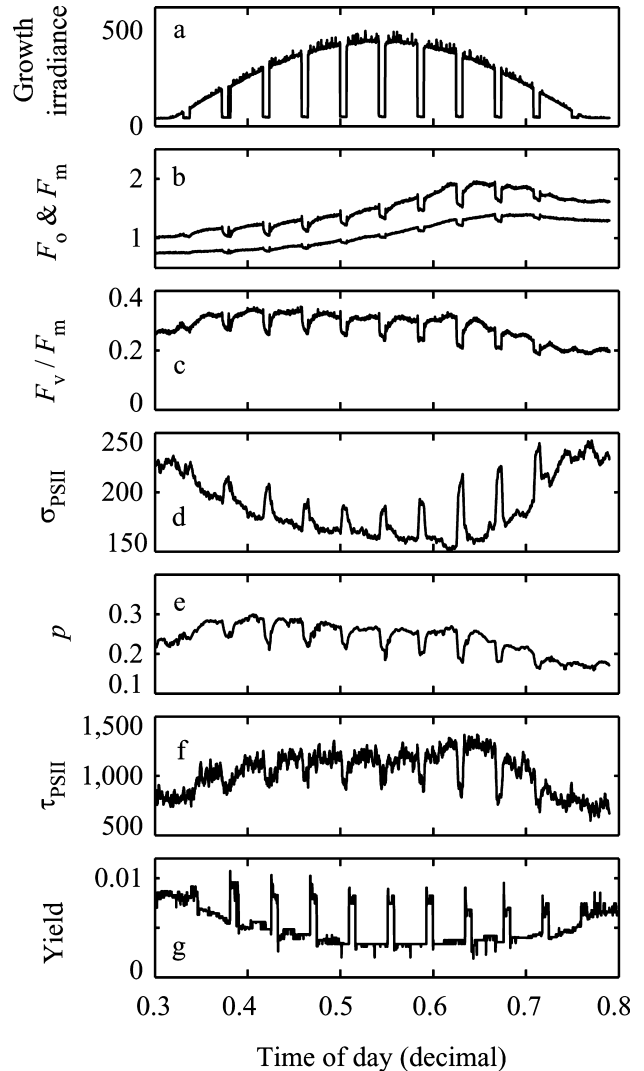


FIG. 11. Growth irradiance (a), measured PSII physiological properties (b–f), and simulated yield of electron flow Φ^P (g) of a nutrient-replete *Thalassiosira weissflogii* culture exposed to brief, transient reductions in growth irradiance. The physiological properties were determined identically as in Figure 9, by continuously passing a portion of the culture through the “dark” chamber of a Fastracka fast repetition rate fluorometer. The transient behavior of these PSII properties, therefore, reflects only the physiological response to these changes in light, not any direct artifact of light levels on the measurement per se. Interpreting these transient responses in PSII in the context of the simulation would suggest that these responses led to increases in Φ^P of 2-fold at most.

was a reasonable proxy for f_{PSII} over the timescale of interest. On other timescales or under other growth conditions, F_v/F_m may not be such an appropriate proxy for f_{PSII} . When the same diatom is grown under intermittent light instead of a steady diurnal cycle (Fig. 11a), rapid transient responses can be observed in many PSII properties including F_v/F_m (Fig. 11, b–f). Incautious analysis of these data using our simulated P_e - E relationships would suggest that these rapid transient responses act to increase the yield of electron flow by as much as 2-fold (Fig. 11g).

A nutrient-replete diatom with the capacity for strong, rapidly reversible energy-dependent quenching (Lavaud et al. 2004) might be expected to alter σ_{PSII} and τ_{PSII} to such a degree, but the concurrent changes in F_v/F_m most probably do not reflect rapid changes in the number of functional PSII's. On these scales, F_v/F_m is probably a poor proxy for f_{PSII} , and the predicted transient increases in Φ^p are questionable.

Finally, it is important to note that there is a wide body of empirical data that present observed relationships between changes in PSII physiology and cotemporal changes in light-driven electron flow. The predictions of a simple dynamical simulation might not be readily reconciled to some of these empirical observations. Our simulation's incomplete description of a complex physiological system is an obvious potential source of such discrepancy, yet in this situation, failures to reconcile model output with observations cannot be attributed solely to models. Empirical studies do not measure all of the relevant physiological factors that control the rates or yield of light-driven electron flow, and a plant or alga's photosynthetic "state" cannot be determined with certainty from a limited number of measured properties. If photon capture and uptake are sufficiently nonlinear at the photosystem level, we can expect that past paradigms for how changes in PSII physiology affect light harvesting may not be as simple as previously thought. The predicted dual role of PSII connectivity as either an enhancer or constrainer of P_e is one such example; presumably, there are others yet to be discovered. An intelligent combination of experimental and modeling approaches may shed valuable insight into how nonlinear interactions in light harvesting arise in actual phytoplankton and which of those interactions are important enough to warrant being incorporated into improved models for P - E . Nonanalytical approaches such as the one presented here have the potential to contribute meaningfully to this synthesis of model and experiment.

We thank Curt Vandetta for valuable administrative support on the computer systems used in this study, and Drs. H. Sosik, C. Miller, P. Wheeler, T. J. Cowles, J. R. V. Zaneveld, and T. Plant for their valuable comments. Suggestions and criticism from an anonymous reviewer helped improve this manuscript considerably. This research was supported in part by the National Aeronautics and Space Administration (NAS5-31360 to M. R. A., and NNG04HZ35C to R. M. L. and M. R. A.), by an Ocean Life Institute Postdoctoral Scholarship to S. R. L. (Woods Hole Oceanographic Institution), and by facilities made available by the Trustees of Deep Springs College.

Abbott, M. R. 1993. Phytoplankton patchiness: ecological implications and observational methods. In Levin, S. A., Powell, T. M. & Steele, J. H. [Eds.] *Patch Dynamics*. Springer-Verlag, Berlin, pp. 37-49.

- Andreo, P. 1991. Monte Carlo techniques in medical radiation physics. *Phys. Med. Biol.* 36:861-920.
- Baly, E. C. C. 1935. The kinetics of photosynthesis. *Proc. R. Soc. Lond. Ser. B* 117:218-39.
- Bannister, T. T. 1979. Quantitative description of steady state, nutrient-saturated algal growth, including adaptation. *Limnol. Oceanogr.* 24:76-96.
- Berner, T., Dubinsky, Z., Wyman, K. & Falkowski, P. G. 1989. Photoadaptation and the package effect in *Dunaliella tertiolecta* (Chlorophyceae). *J. Phycol.* 25:70-8.
- Bernhardt, K. & Trissl, H.-W. 1999. Theories for kinetics and yields of fluorescence and photochemistry: how, if at all, can different models of antenna organization be distinguished experimentally? *Biochim. Biophys. Acta* 1409:125-42.
- Cullen, J. J. 1990. On models of growth and photosynthesis in phytoplankton. *Deep-Sea Res.* 37:667-83.
- Dubinsky, Z., Falkowski, P. G. & Wyman, K. 1986. Light harvesting and utilization in phytoplankton. *Plant Cell Physiol.* 27:1335-49.
- Falkowski, P. G. 1992. Molecular ecology of phytoplankton photosynthesis. In Falkowski, P. G. & Woodhead, A. D. [Eds.] *Primary Productivity and Biogeochemical Cycles in the Sea*. Plenum Press, New York, pp. 47-68.
- Falkowski, P. G. & Kolber, Z. 1993. Estimation of phytoplankton photosynthesis by active fluorescence. *ICES Mar. Sci. Symp.* 197:92-103.
- Falkowski, P. G. & Kolber, Z. S. 1995. Variations in chlorophyll fluorescence yields in phytoplankton in the world oceans. *Aust. J. Plant Physiol.* 22:341-55.
- Falkowski, P. G., Kolber, Z. & Fujita, Y. 1988. Effect of redox state on the dynamics photosystem II (sic) during steady-state photosynthesis in eucaryotic algae. *Biochim. Biophys. Acta* 933:432-43.
- Falkowski, P. G. & LaRoche, J. 1991. Acclimation to spectral irradiance in algae. *J. Phycol.* 27:8-14.
- Falkowski, P. G. & Raven, J. A. 1997. *Aquatic Photosynthesis*. Blackwell Science, Malden, Massachusetts, 375 pp.
- Fragata, M. & Dudekula, S. 2005. Nonlinear enhancement of oxygen evolution in thylakoid membranes: modeling the effect of light intensity and β -cyclodextrin concentration. *J. Phys. Chem. B* 109:14707-14.
- Franks, P. J. S. 2002. NPZ models of plankton dynamics: their construction, coupling to physics, and application. *J. Oceanogr.* 58:379-87.
- Furukawa, T., Watanabe, M. & Shihira-Ishikawa, I. 1998. Green- and blue-light-mediated chloroplast migration in the centric diatom *Pleurosira laevis*. *Protoplasma* 203:214-20.
- Glass, L. 2001. Synchronization and rhythmic processes in physiology. *Nature* 410:277-84.
- Gorbunov, M. Y., Kolber, Z. S. & Falkowski, P. G. 2000. Measurement of photosynthetic parameters in benthic organisms in situ using a SCUBA-based fast repetition rate fluorometer. *Limnol. Oceanogr.* 45:242-5.
- Han, B.-P. 2001. Photosynthesis-irradiance response at physiological level: a mechanistic model. *J. Theor. Biol.* 213:121-7.
- Huot, Y., Brown, C. A. & Cullen, J. J. 2005. New algorithms for MODIS sun-induced chlorophyll fluorescence and a comparison with present data products. *Limnol. Oceanogr. Meth.* 3:108-30.
- Jassby, A. D. & Platt, T. 1976. Mathematical formulation of the relationship between photosynthesis and light for phytoplankton. *Limnol. Oceanogr.* 21:540-7.
- Joliot, P. & Joliot, A. 1964. Études cinétique de la réaction photochimique libérant l'oxygène au cours de la photosynthèse. *C. R. Acad. Sci. Paris* 258:4622-5.
- Kaftan, D., Meszaros, T., Whitmarsh, J. & Nedbal, L. 1999. Characterization of photosystem II activity and heterogeneity during the cell cycle of the green alga *Scenedesmus quadricauda*. *Plant Physiol.* 120:433-42.
- Kevekedis, I. G., Gear, C. W. & Hummer, G. 2004. Equation-free: the computer-aided analysis of complex multiscale systems. *AIChE J.* 50:1346-55.

- Kim, J. H., Glick, R. E. & Melis, A. 1993. Dynamics of photosystem stoichiometry adjustment by light quality in chloroplasts. *Plant Physiol.* 102:181–90.
- Kolber, Z. S. & Falkowski, P. G. 1992. Fast repetition rate fluorometer for making in situ measurements of primary productivity. In *Proceedings of IEEE Ocean 92 Conference*. Newport, Rhode Island. IEEE, New York, pp. 637–41.
- Kolber, Z. S. & Falkowski, P. G. 1993. Use of active fluorescence to estimate phytoplankton photosynthesis in situ. *Limnol. Oceanogr.* 38:1646–65.
- Kolber, Z. S., Prasil, O. & Falkowski, P. G. 1998. Measurements of variable chlorophyll fluorescence using fast repetition rate techniques: defining methodology and experimental protocols. *Biochim. Biophys. Acta* 1367:88–106.
- Korn, R. 2005. The emergence principle in biological hierarchies. *Biol. Philos.* 20:137–51.
- Kromkamp, J. C. & Forster, R. M. 2003. The use of variable fluorescence measurements in aquatic ecosystems: differences between multiple and single turnover measuring protocols and suggested terminology. *Eur. J. Phycol.* 38:103–22.
- Kroon, B. M. A. & Thoms, S. 2006. From electron to biomass: a mechanistic model to describe phytoplankton photosynthesis and steady-state growth rates. *J. Phycol.* 42:593–609.
- Laney, S. R. 2003. Assessing the error in photosynthetic properties determined by fast repetition rate fluorometry. *Limnol. Oceanogr.* 48:2234–42.
- Laney, S. R. & Letelier, R. M. 2008. Artifacts in measurements of chlorophyll fluorescence transients, with specific application to fast repetition rate fluorometry. *Limnol. Oceanogr. Meth.* 6:40–50.
- Laney, S. R., Letelier, R. M. & Abbott, M. R. 2005. Parameterizing the natural fluorescence kinetics of *Thalassiosira weissflogii*. *Limnol. Oceanogr.* 50:1499–510.
- Lavaud, J., Rousseau, B. & Etienne, A.-L. 2004. General features of photoprotection by energy dissipation in planktonic diatoms (Bacillariophyceae). *J. Phycol.* 40:130–7.
- Lavorel, J. 1986. A Monte Carlo method for the simulation of kinetic models. *Photosynth. Res.* 9:273–83.
- Maskell, E. J. 1928. Experimental researches on vegetable assimilation and respiration. XVIII. The relation between stomatal opening and assimilation – a critical study of assimilation rates and porometer rates in leaves of cherry laurel. *Proc. R. Soc. Lond. Ser. B* 102:488–533.
- May, R. M. 1976. Simple mathematical models with very complicated dynamics. *Nature* 261:459–67.
- Nedbal, L. & Březina, V. 2002. Complex metabolic oscillations in plants forced by harmonic irradiance. *Biophys. J.* 83:2180–9.
- Nedbal, L., Březina, V., Adamec, F., Štys, D., Oja, V., Laisk, A. & Govindjee 2003. Negative feedback regulation is responsible for the non-linear modulation of photosynthetic activity in plants and cyanobacteria exposed to a dynamic light environment. *Biochim. Biophys. Acta* 1607:5–17.
- Nedbal, L., Březina, V., Červený, J. & Trtílek, M. 2005. Photosynthesis in dynamic light: systems biology of unconventional chlorophyll fluorescence transients in *Synechocystis* sp. PCC 6803. *Photosynth. Res.* 84:99–106.
- Parkhill, J.-P., Maillet, G. & Cullen, J. J. 2001. Fluorescence-based maximal quantum yield for PSII as a diagnostic of nutrient stress. *J. Phycol.* 37:517–29.
- Platt, T., Gallegos, C. L. & Harrison, W. G. 1980. Photoinhibition of photosynthesis and light for natural assemblages of coastal marine phytoplankton. *J. Mar. Res.* 38:687–701.
- Press, W. H., Teukolsky, S. A., Vetterling, W. T. & Flannery, B. P. 1992. *Numerical Recipes in C*. Cambridge University Press, Cambridge, 1020 pp.
- Rascher, U. & Nedbal, L. 2006. Dynamics of photosynthesis in fluctuating light. *Curr. Opin. Plant Biol.* 9:671–8.
- Samson, G., Prášíl, O. & Yaakoubd, B. 1999. Photochemical and thermal phases of chlorophyll *a* fluorescence. *Photosynthetica* 37:163–82.
- Smith, E. L. 1936. Photosynthesis in relation to light and carbon dioxide. *Proc. Natl. Acad. Sci.* 22:504–11.
- Strasser, R. J., Srivastava, A. & Govindjee 1995. Polyphasic chlorophyll *a* fluorescence transient in plants and cyanobacteria. *Photochem. Photobiol.* 61:32–42.
- Strogatz, S. H. 1994. *Nonlinear Dynamics and Chaos: With Applications to Physics, Biology, Chemistry, and Engineering*. Addison-Wesley, Reading, Massachusetts, 198 pp.
- Strogatz, S. H. 2001. Exploring complex networks. *Nature* 410:277–84.
- Suggett, D., Kraay, G., Holligan, P., Davey, M., Aiken, J. & Geider, R. 2001. Assessment of photosynthesis in a spring cyanobacterial bloom by use of a fast repetition rate fluorometer. *Limnol. Oceanogr.* 46:802–10.
- Sukenik, A., Falkowski, P. G. & Bennett, J. 1987. Potential enhancements of photosynthetic energy conversion in algal mass culture. *Biotech. Bioeng.* 30:970–7.
- Thornley, J. H. M. 1998. Dynamic model of leaf photosynthesis with acclimation to light and nitrogen. *Ann. Bot.* 81:421–30.
- Webb, W. L., Newton, M. & Starr, D. 1974. Carbon dioxide exchange of *Alnus rubra*: a mathematical model. *Oecologia (Berl.)* 17:281–91.
- Zhu, X.-G., Govindjee, Baker, N. R., deSturler, E., Ort, D. R. & Long, S. P. 2005. Chlorophyll *a* fluorescence induction kinetics in leaves predicted from a model describing each discrete step of excitation energy and electron transfer associated with photosystem II. *Planta* 223:114–33.